Robust features of the source process for the 2004 Parkfield, California, earthquake from strong-motion seismograms

(submitted to GJI: under revision)

C. Twardzik
Oxford University

Motivation

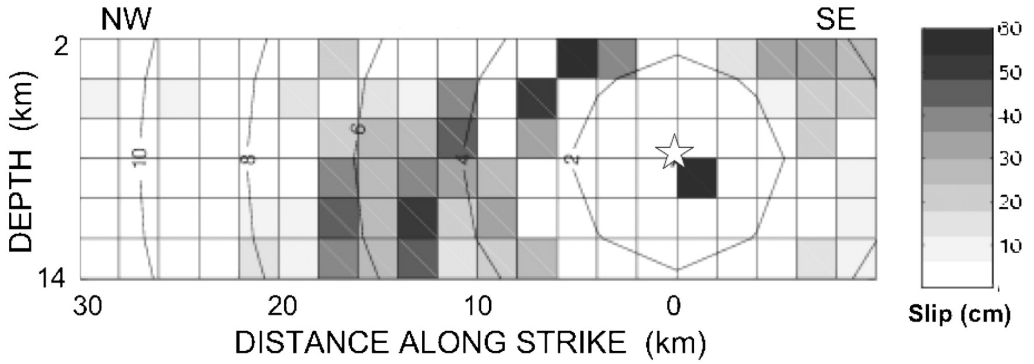

C. Mendoza and S. Hartzell, 2008
P_{nl} waveforms

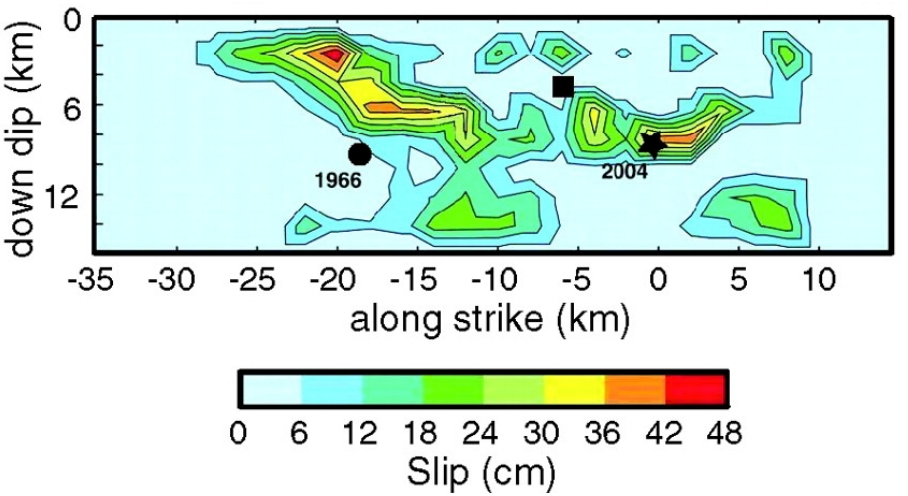

P. Liu et al., 2006
Strong-motion data

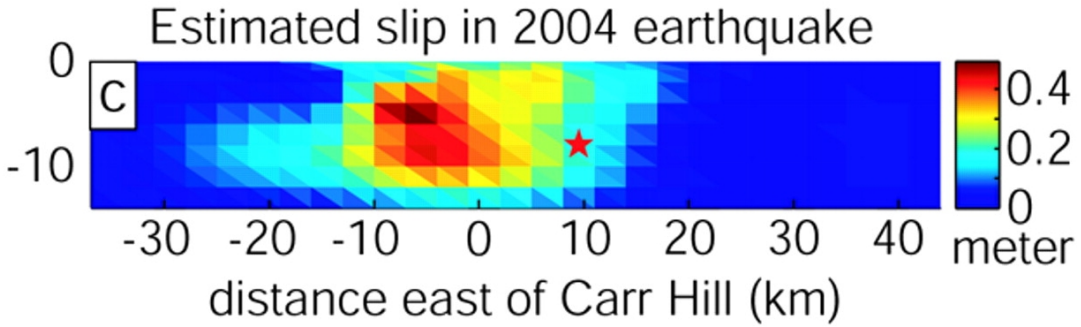

J. Murray and J. Langbein, 2006
GPS data

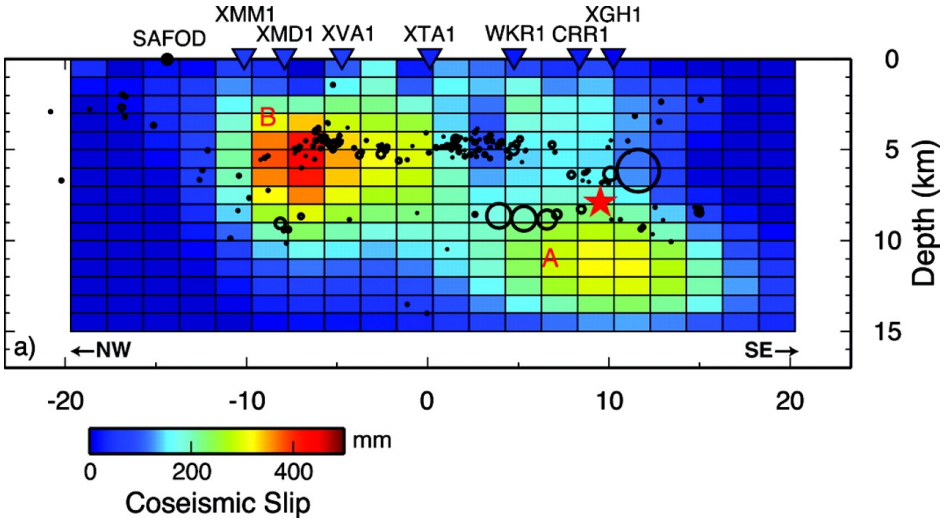

Johanson et al., 2006
InSAR and GPS

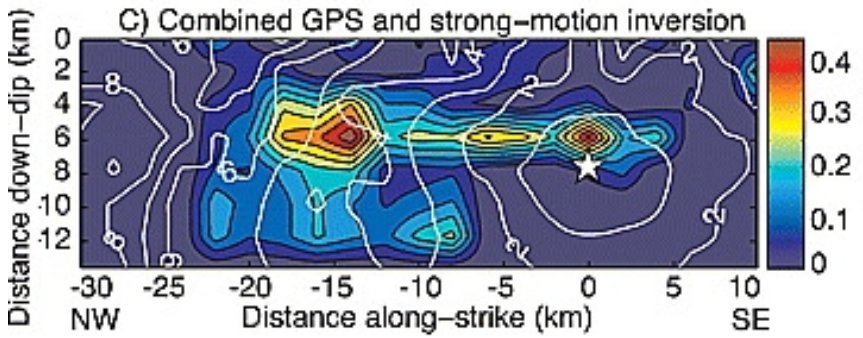

S. Custodio et al., 2009
Strong-motion and GPS

Elliptical sub-fault approximation

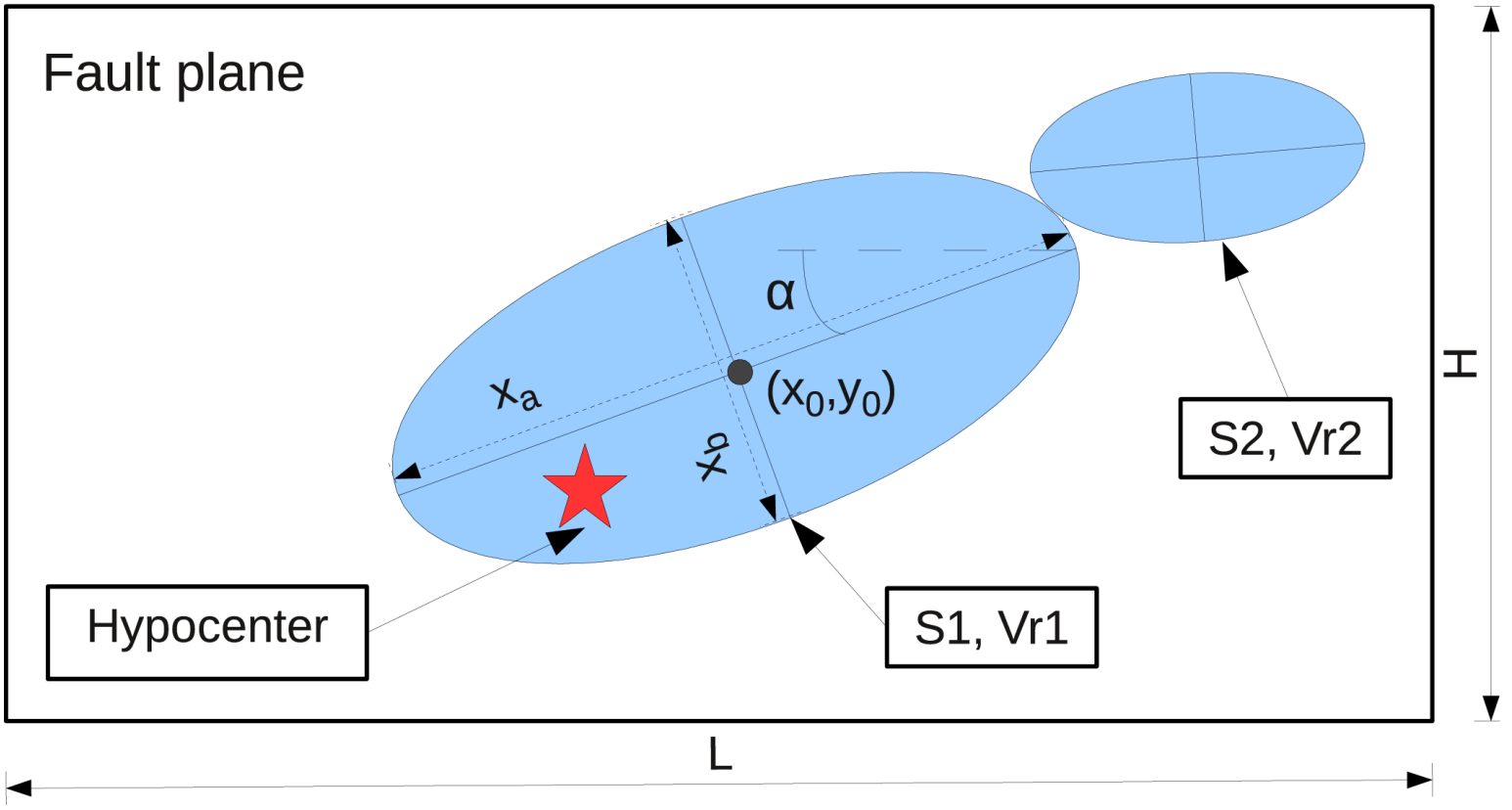

Elliptical sub-fault approximation

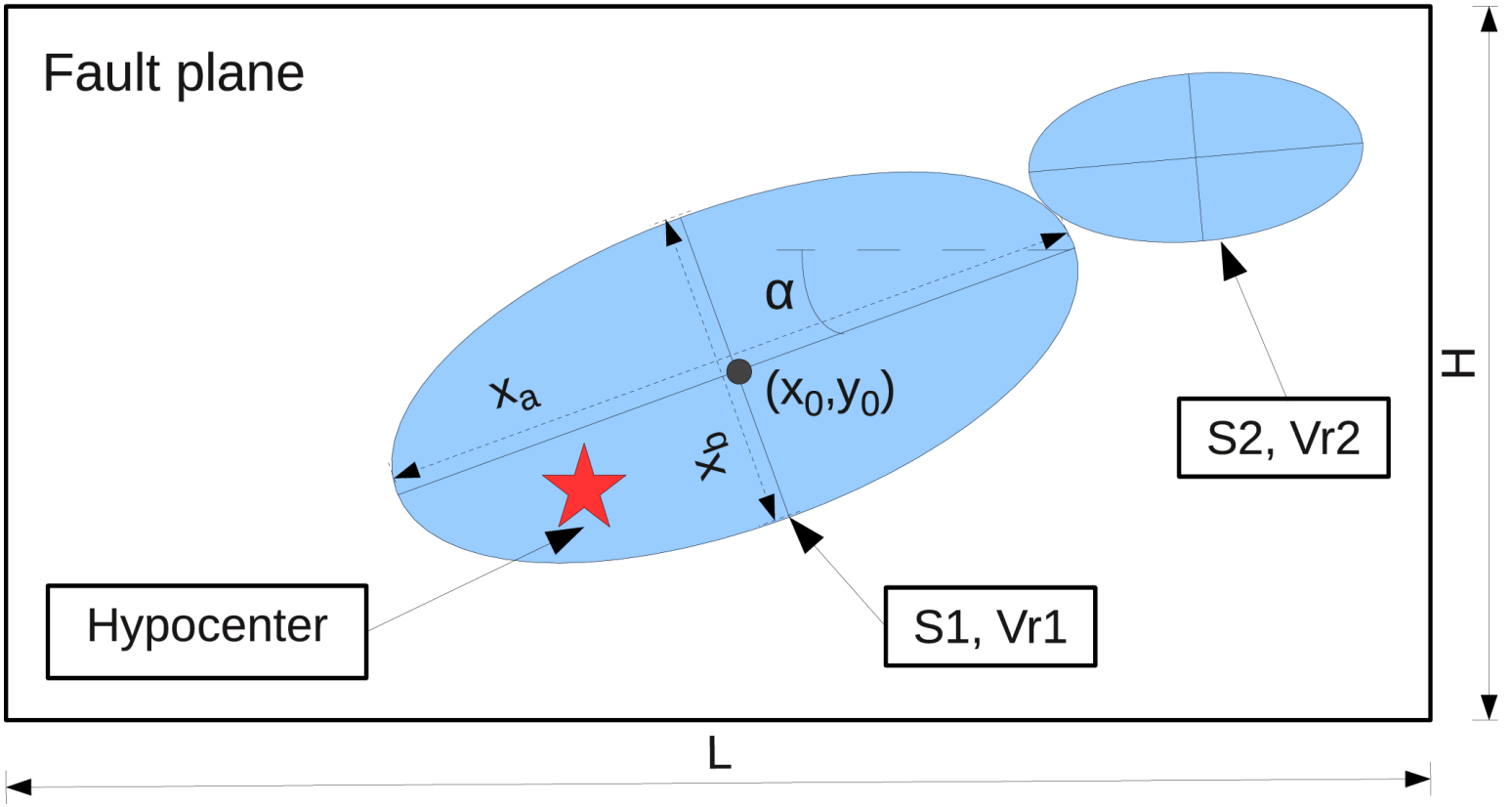

“This is why we propose a global method […] to identify the most robust features of large earthquake source processes” - Vallée and Bouchon, 2004

Calculation of seismograms

$$u_k(t) = s(t) * g_k(t) * i_k(t)$$

Calculation of seismograms

$$u_k(t) = s(t) * g_k(t) * i_k(t)$$

Source processes

Calculation of seismograms

$$u_k(t) = s(t) * g_k(t) * i_k(t)$$

Calculation of seismograms

$$u_k(t) = s(t) * g_k(t) * i_k(t)$$

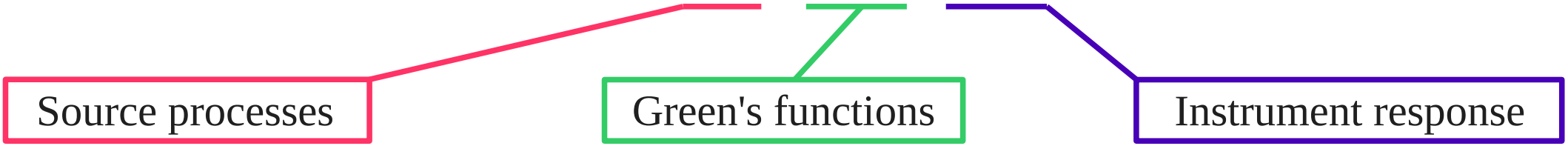

Calculation of seismograms

$$u_k(t) = s(t) * g_k(t) * i_k(t)$$

Source processes

Green's functions

Instrument response

In the inversion, we used this representation:

$$u_n(\boldsymbol{x}, t) = \int_{-\infty}^{+\infty} d\tau \int\int_{\Sigma} \left[u_i(\zeta, \tau) \right] . \nu_i . C_{ijkl} . \frac{\partial}{\partial \zeta_q} G_{np}(\boldsymbol{x}, t - \tau, \zeta, 0) \, d\Sigma$$

Calculation of seismograms

$$u_k(t) = s(t) * g_k(t) * i_k(t)$$

Source processes

Green's functions

Instrument response

In the inversion, we used this representation:

$$u_n(\boldsymbol{x},t) = \int_{-\infty}^{+\infty} d\tau \int\int_{\Sigma} \left[u_i(\zeta,\tau)\right] . \nu_i . C_{ijkl} . \frac{\partial}{\partial \zeta_q} G_{np}(\boldsymbol{x}, t-\tau, \zeta, 0)\, d\Sigma$$

Calculation of the Green's function:

- Spectral discrete wave number integration method (Bouchon, 1981)

- Reflections/Transmissions within the layered medium is computed using the reflectivity algorithm of Kerry and Kennett, 1979

The 2004 Parkfield earthquake

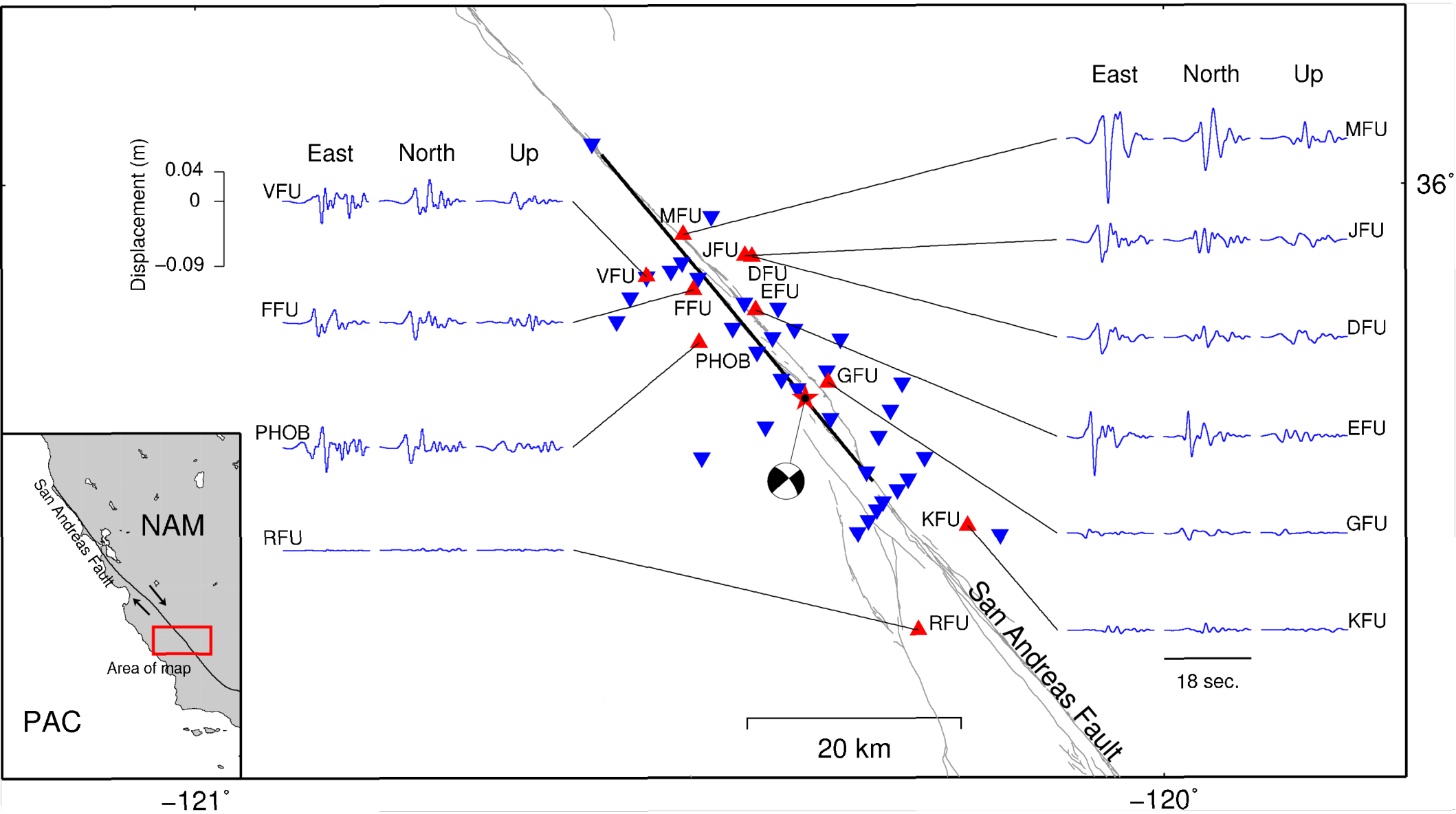

Freq. Band: 0.16Hz to 1Hz

Synthetic test

Synthetic test

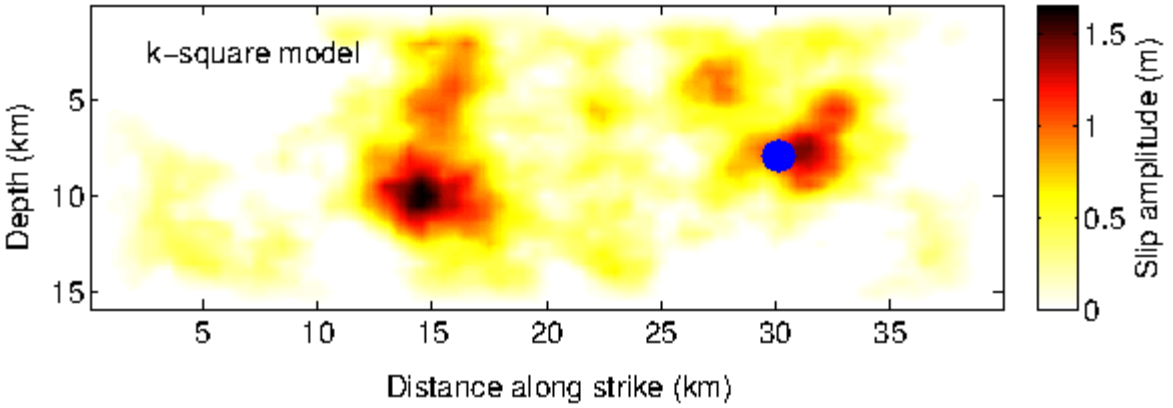

We used a k^{-2} type, double asperity, slip distribution

Synthetic test

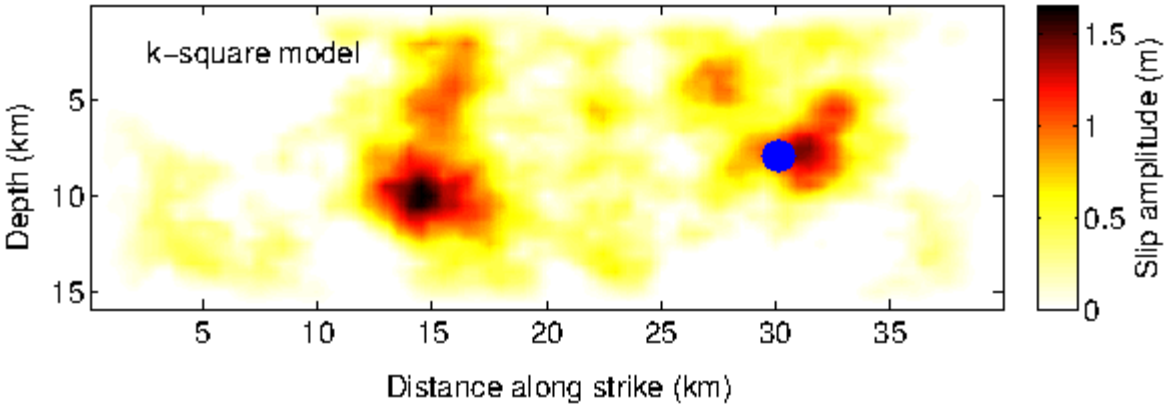

We used a k^{-2} type, double asperity, slip distribution

We propagate a rupture front at
v_r = 3.0 km/s

Synthetic test

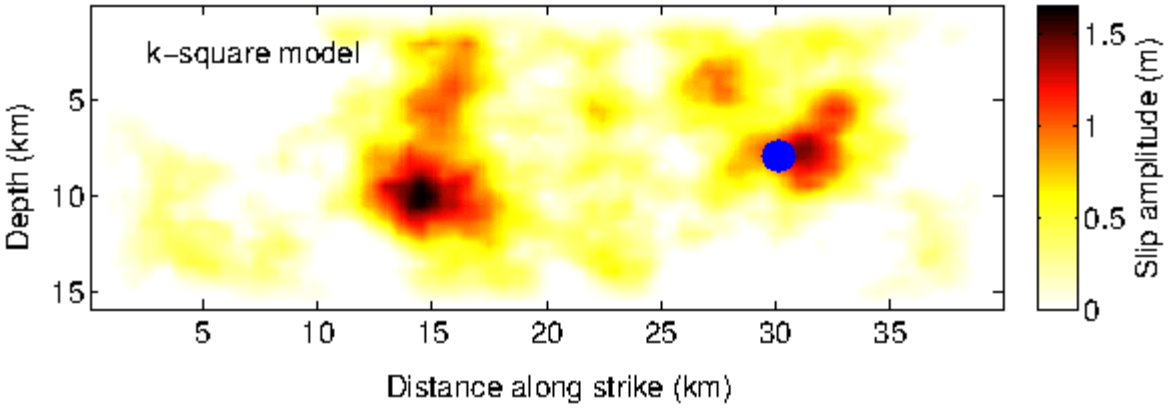

We used a k^{-2} type, double asperity, slip distribution

We propagate a rupture front at $v_r = 3.0$ km/s

We generate artificial data

Synthetic test

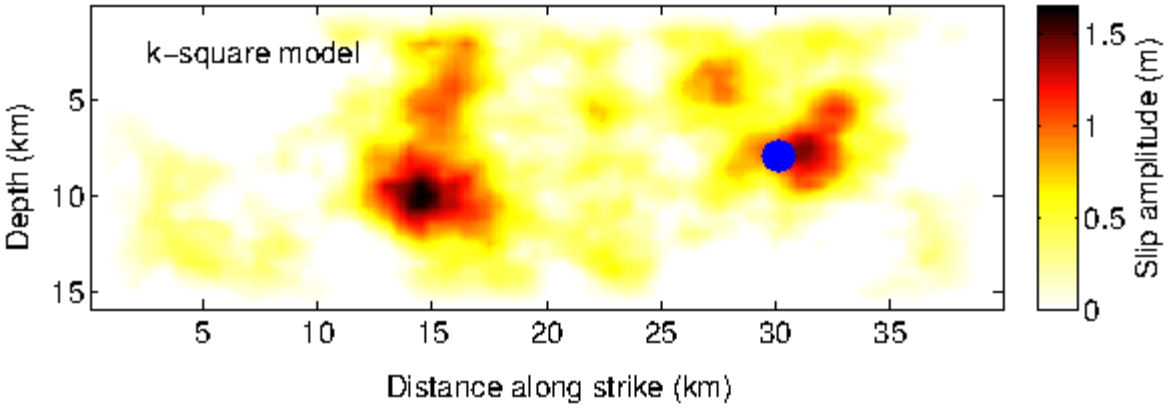

We used a k^{-2} type, double asperity, slip distribution

We propagate a rupture front at $v_r = 3.0$ km/s

We generate artificial data

Inversion using one ellipse

Synthetic test

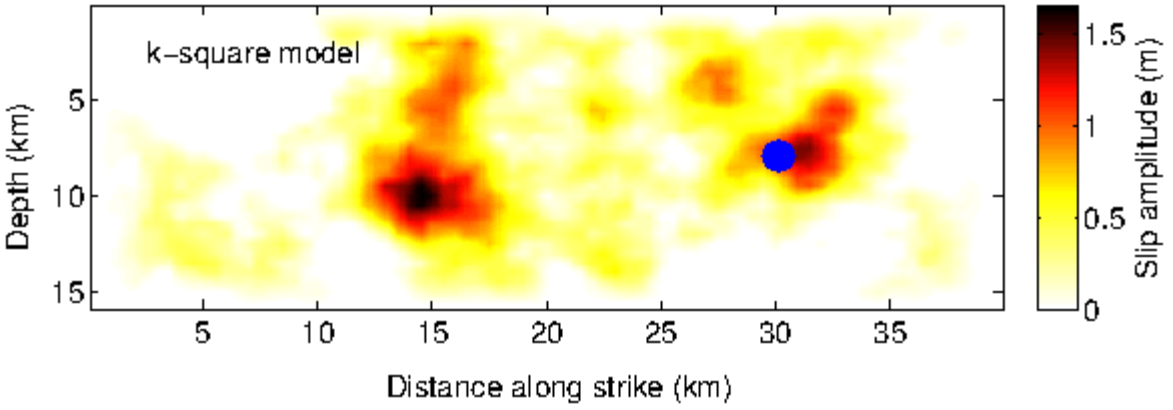

We used a k^{-2} type, double asperity, slip distribution

We propagate a rupture front at $v_r = 3.0$ km/s

We generate artificial data

- Inversion using one ellipse
- Inversion using two ellipses

One ellipse

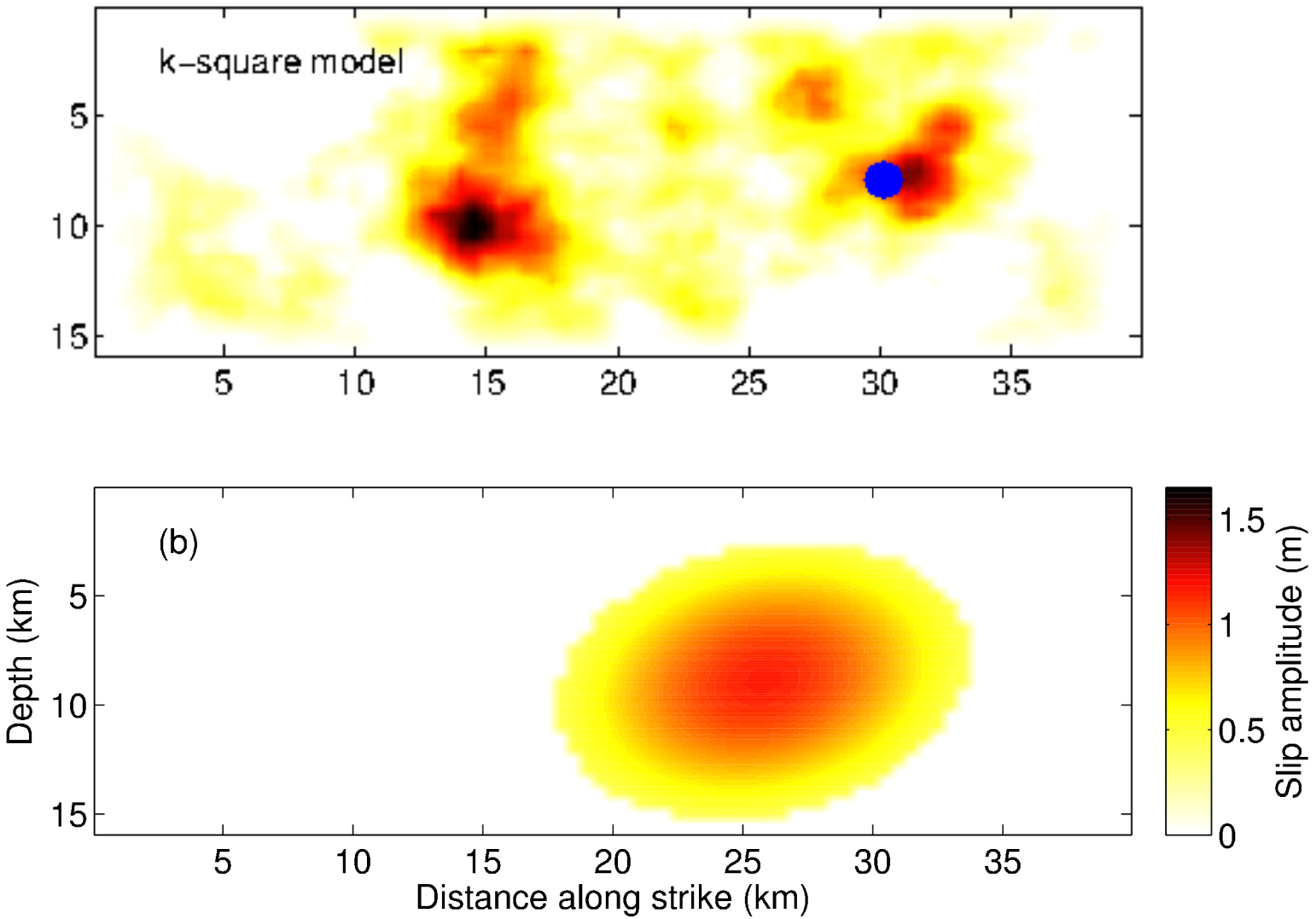
k−square model
5
10
15
5
10
15
20
25
30
35
(b)
Depth (km)
5
10
15
5
10
15
20
25
30
35
Distance along strike (km)
1.5
1
0.5
0
Slip amplitude (m)

One ellipse

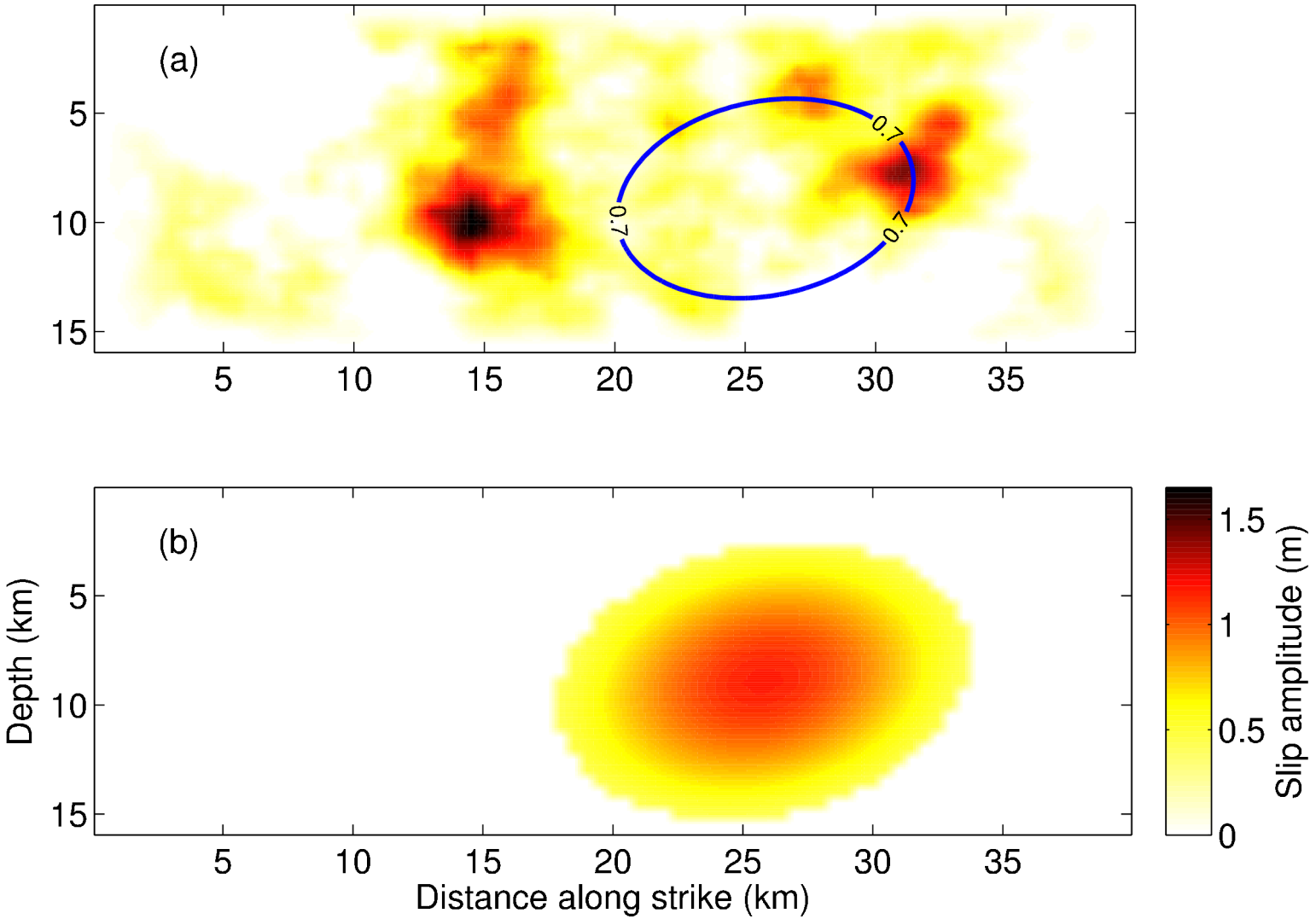
(a)
(b)
0.7
0.7
0.7
5
10
15
20
25
30
35
Depth (km)
Distance along strike (km)
1.5
1
0.5
0
Slip amplitude (m)

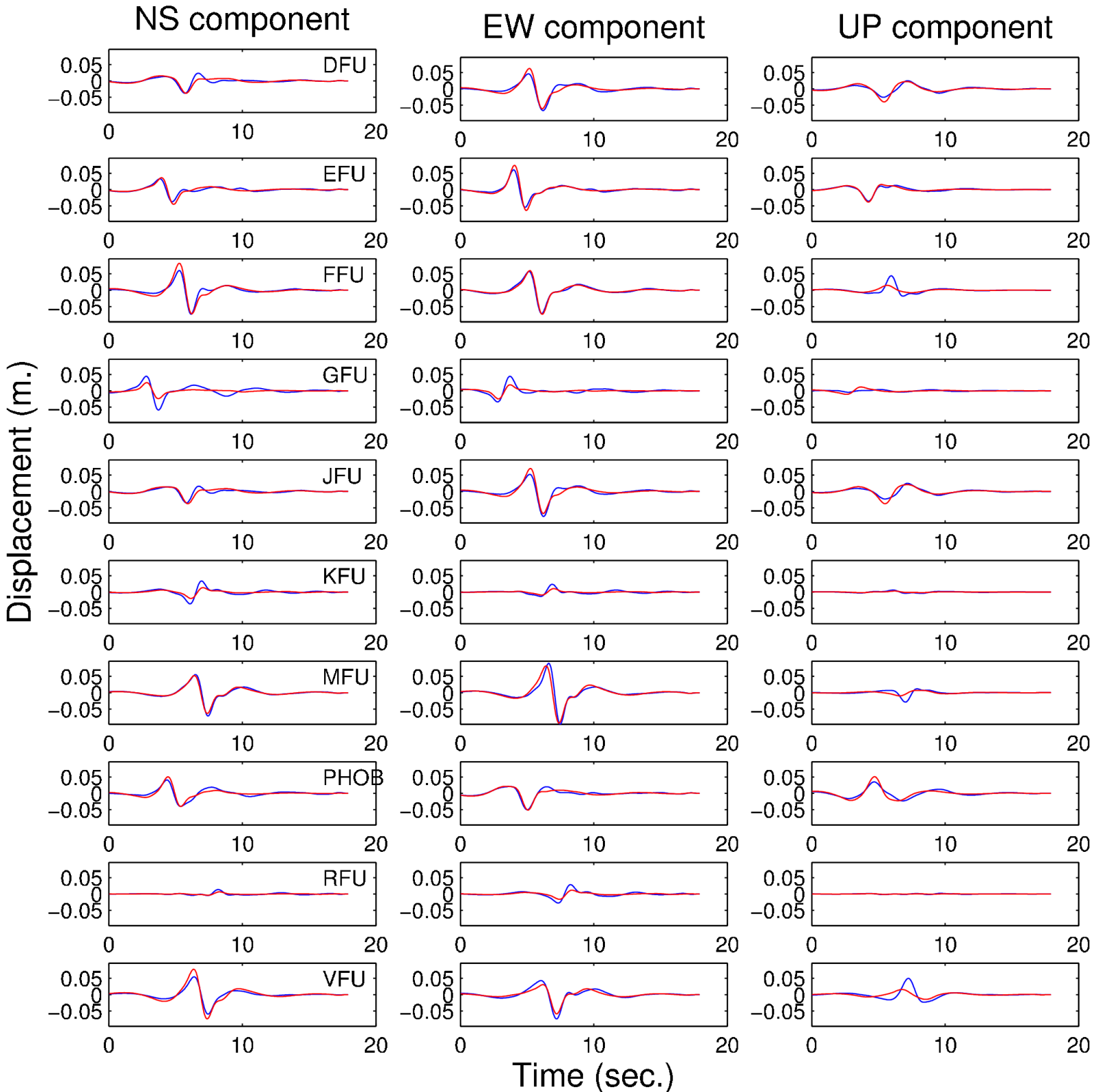
NS component
EW component
UP component
Displacement (m.)
Time (sec.)
DFU
EFU
FFU
GFU
JFU
KFU
MFU
PHOB
RFU
VFU
0.05
0
−0.05
0
10
20

Two ellipses

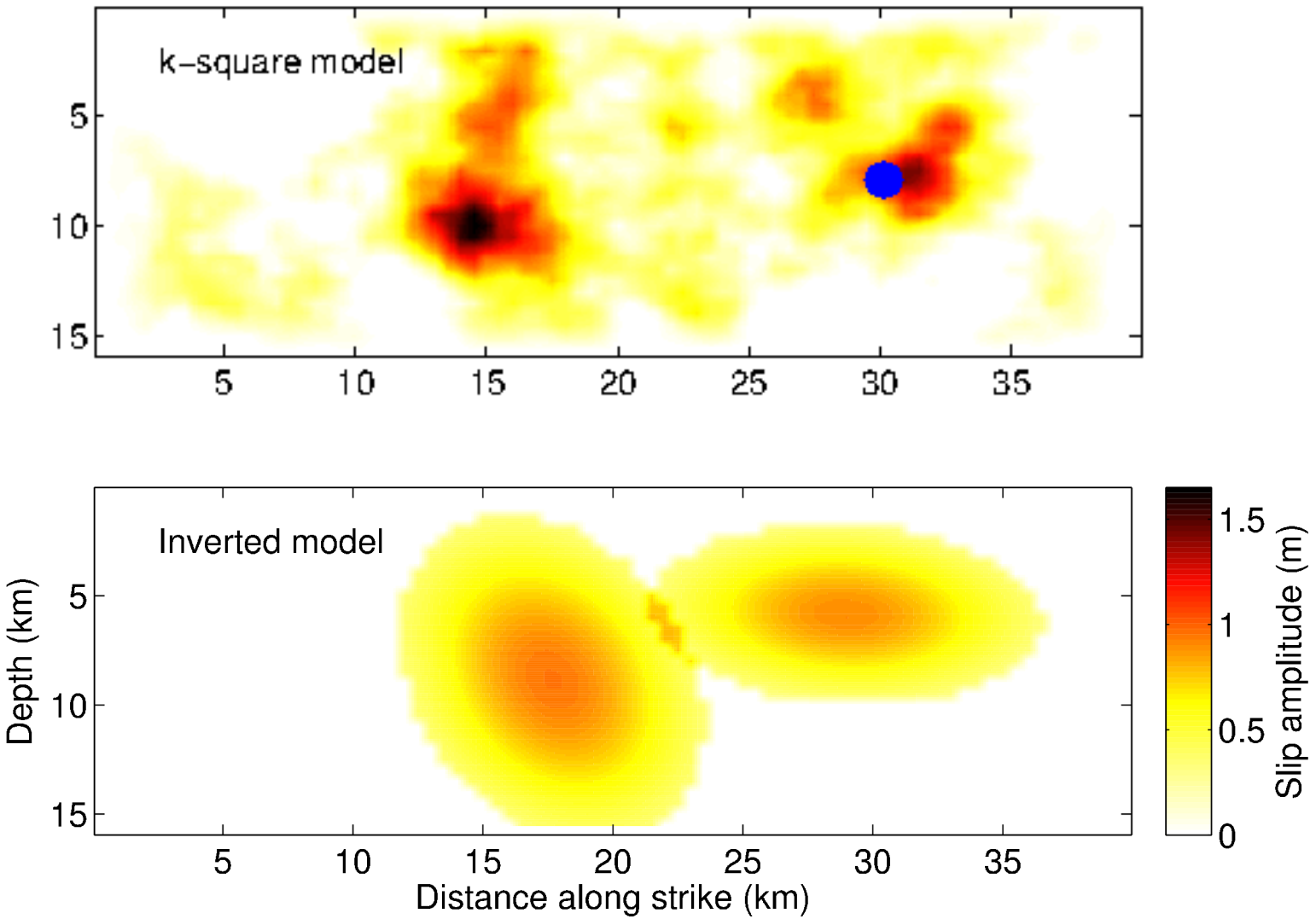

Two ellipses

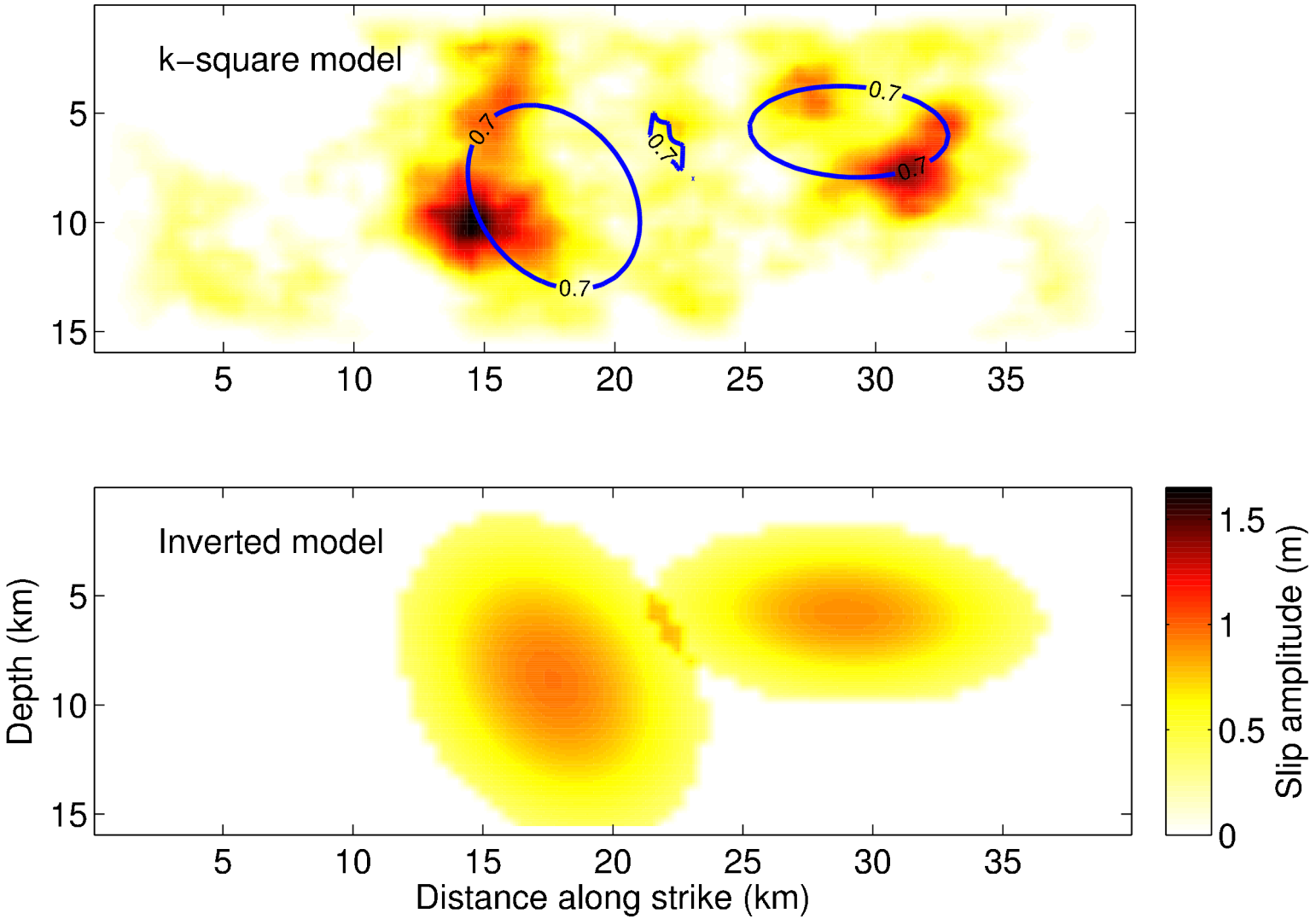

Summary of all inversions carried out

Table 1. Summary of the rupture process for the 12 inversions. Detailed results on each parameter for the 12 inversions are shown in Supplementary Materials.

Inversion	Set-up of the inversion	Summary of the rupture process
Inversion 1	Inversion using two connected ellipses; use of *a-priori* conditions; The rise-time and rake were not inverted	Misfit for the digital stations: 0.27; Misfit for the analog stations: 0.52; Moment: 1.78 $\times$ 10^{18} N.m; The rupture front propagates mostly in the forward direction at a speed of 3.00 km/s. A propagation of the rupture front in the backward direction is also observed for the first 1.7 sec. About 4.5 sec. after the start of the process, the high slip amplitude patch starts to break at a slightly higher rupture speed (3.30 km/s). The whole process is finished after 10.6 sec. of rupture.
Inversion 2	Inversion using two connected ellipses; No use of *a-priori* conditions; The rise-time and rake were inverted	Misfit for the digital stations: 0.30; Misfit for the analog stations: 0.54; Moment: 1.13 $\times$ 10^{18} N.m; No backward propagation is observed for this inversion. The rupture front reaches the peak of slip amplitude almost instantaneously (0.8 sec. after the start of the earthquake) at a really high rupture speed (4.96 km/s). This hypocentral patch finishes rupturing about 1.3 sec. later. The rupture front then propagates across the second ellipse at a slower speed (3.36 km/s). 5.8 sec. are needed by the rupture front to break all asperities.
Inversion 3	Inversion using two disconnected ellipses; No use of *a-priori* conditions; The rise-time and rake were inverted	Misfit for the digital stations: 0.28; Misfit for the analog stations: 0.50; Moment: 2.03 $\times$ 10^{18} N.m; We observed a bilateral propagation of the rupture front for about 2.5 sec., which is about the time taken to rupture the all hypocentral asperity (2.9 sec.). In this first part, the rupture starts at a low rupture speed of 2.15 km/s. Almost straight after that, the second ellipse start to rupture at higher speed (3.51 km/s). The whole process takes about 9.3 sec., when the rupture front reaches the end of the fault plane.
Inversion 4	Inversion using two connected ellipses; use of *a-priori* conditions; The rise-time and rake were inverted	Misfit for the digital stations: 0.30; Misfit for the analog stations: 0.59; Moment: 1.56 $\times$ 10^{18} N.m; For this inversion, we observed a bilateral propagation of the rupture front at a speed of 3.8 km/s. In the backward direction, the rupture front reaches the end of the fault about 3.6 sec. after the initiation of the earthquake. In the forward direction, the high amplitude slip patch starts to break after 5.0 sec and ruptures at a speed of 2.98 km/s. It takes 10.7 sec. for the whole process to be achieved.
Inversion 5	Inversion using two connected ellipses; use of *a-priori* conditions; The rise-time and rake were not inverted	Misfit for the digital stations: 0.28; Misfit for the analog stations: 0.53; Moment: 1.14 $\times$ 10^{18} N.m; The rupture front starts to propagate bilaterally for about 2.4 sec. Then it only propagates in the forward direction at a speed of about 2.5-3.0 km/s. The peak of amplitude of the second ellipse is reached by the rupture front about 3.3 sec. after the start of the earthquake. After 7.9 sec., the process is terminated.
Inversion 6 PREFERRED MODEL	**Inversion using two disconnected ellipses; No use of *a-priori* conditions; The rise-time and rake were not inverted**	**Misfit for the digital stations: 0.26; Misfit for the analog stations: 0.56; Moment: 1.21 $\times$ 10^{18} N.m; For this inversion, the rupture is only propagating in the forward direction. It takes 3.2 sec. for the first ellipse to be break at a slow rupture speed of 2.2 km/s. After 3.8 sec. the rupture front reaches the second ellipse. The rupture front slightly accelerates to a speed of 3.1 km/s. After 8.2 sec., the second ellipse is entirely broken. For this inversion, we also calculated the stress drop associated with each ellipse. The stress drop is about 15 MPa for the hypocentral ellipse, and 17 MPa for the second ellipse.**
Inversion 7	Inversion using two connected ellipses; No use of *a-priori* conditions; The rise-time and rake were not inverted	Misfit for the digital stations: 0.30; Misfit for the analog stations: 0.55; Moment: 2.08 $\times$ 10^{18} N.m; A backward propagation of the rupture front is observed at the very beginning (first 1.5 sec.), but mostly propagates in the forward direction. As the first ellipse is almost non-existent in term of amplitude, we can consider that the rupture front only propagates at the speed of the second ellipse (3.4 km/s). The peak of slip amplitude of the second ellipse is reached by the rupture front about about 3.2 sec. after the earthquakes initiated. The process then stops after 9.5 sec.
Inversion 8	Inversion using two disconnected ellipses; use of *a-priori* conditions; The rise-time and rake were inverted	Misfit for the digital stations: 0.26; Misfit for the analog stations: 0.57; Moment: 1.20 $\times$ 10^{18} N.m; In this inversion, the rupture front propagates only the forward direction. It breaks the first asperity at a rupture speed of 2 km/s and takes about 3.2 sec. to get across the ellipse. Then, the second asperity starts rupturing after 3.6 sec. It takes 4.2 sec to finish breaking the second asperity at a speed of 3.6 km/s.
Inversion 9	Inversion using two disconnected ellipses; use of *a-priori* conditions; The rise-time and rake were not inverted; We forced each model to have some slip the the hypocenter	Misfit for the digital stations: 0.28; Misfit for the analog stations: 0.67; Moment: 1.90 $\times$ 10^{18} N.m; In this inversion, the rupture front propagates in the forward direction, breaking the first asperity after 2.3 sec at a speed of 2.00 km/s. Then, the second asperity starts rupturing after 3.4 sec. The rupture front then propagates at higher speed (3.1 km/s) It takes 7 sec to finish breaking the second asperity and terminate the process, when the rupture front reaches the end of the fault plane.
Inversion 10	Inversion using two connected ellipses; use of *a-priori* conditions; The rise-time and rake were not inverted; We constrain the moment to be within +/−15% of the CMT value	Misfit for the digital stations: 0.29; Misfit for the analog stations: 0.53; Moment: 1.22 $\times$ 10^{18} N.m; We observed only a forward propagating of the rupture front for this inversion. The hypocentral high amplitude slip patch starts to break after 0.9 sec, at a speed of 2.3 km/s. The rupture front gets across it 0.6 sec. later. Then it breaks the second ellipse at a speed of 3.1 km/s,reaching its peak of slip amplitude about 3.5 sec. after the earthquake initiation. 7.8 sec. of rupture, are needed before the process stops.
Inversion 11	Inversion using two connected ellipses; use of *a-priori* conditions; The rise-time and rake were not inverted; The 1D velocity model of the south-western side were used	Misfit for the digital stations: 0.34; Misfit for the analog stations: 0.63; Moment: 1.92 $\times$ 10^{18} N.m; During the first 2.5 sec., the rupture front propagates bilaterally and then propagates only in the forward direction. After 5 sec., the rupture front reaches the high slip amplitude patch and breaks it until it reaches the end of the fault plane after 9.8 sec. of process. The rupture speed is nearly constant in the whole process (3.1-3.3 km/s)
Inversion 12	Inversion using three connected ellipses; use of *a-priori* conditions; The rise-time and rake were not inverted;	Misfit for the digital stations: 0.26; Misfit for the analog stations: 0.60; Moment: 2.71 $\times$ 10^{18} N.m; The rupture front propagates bilaterally in the first ellipse at a speed of 2 km/s. After 2.0 sec., the first ellipse is entirely broken. The rupture front continues to propagate through the second ellipse at a speed of 3.4 km/s. 4 sec. after the earthquake initiation, the rupture front reaches the high slip amplitude patch. It then takes about 5 sec. before the rupture front breaks the high slip patch and reaches the end of the fault plane. The small slip amplitude patch, surrounding the high slip patch breaks at a slightly lower rupture speed (2.8 km/s). The process is finished 11 sec. after the start of the earthquake.

Final slip distribution of the 12 inversions

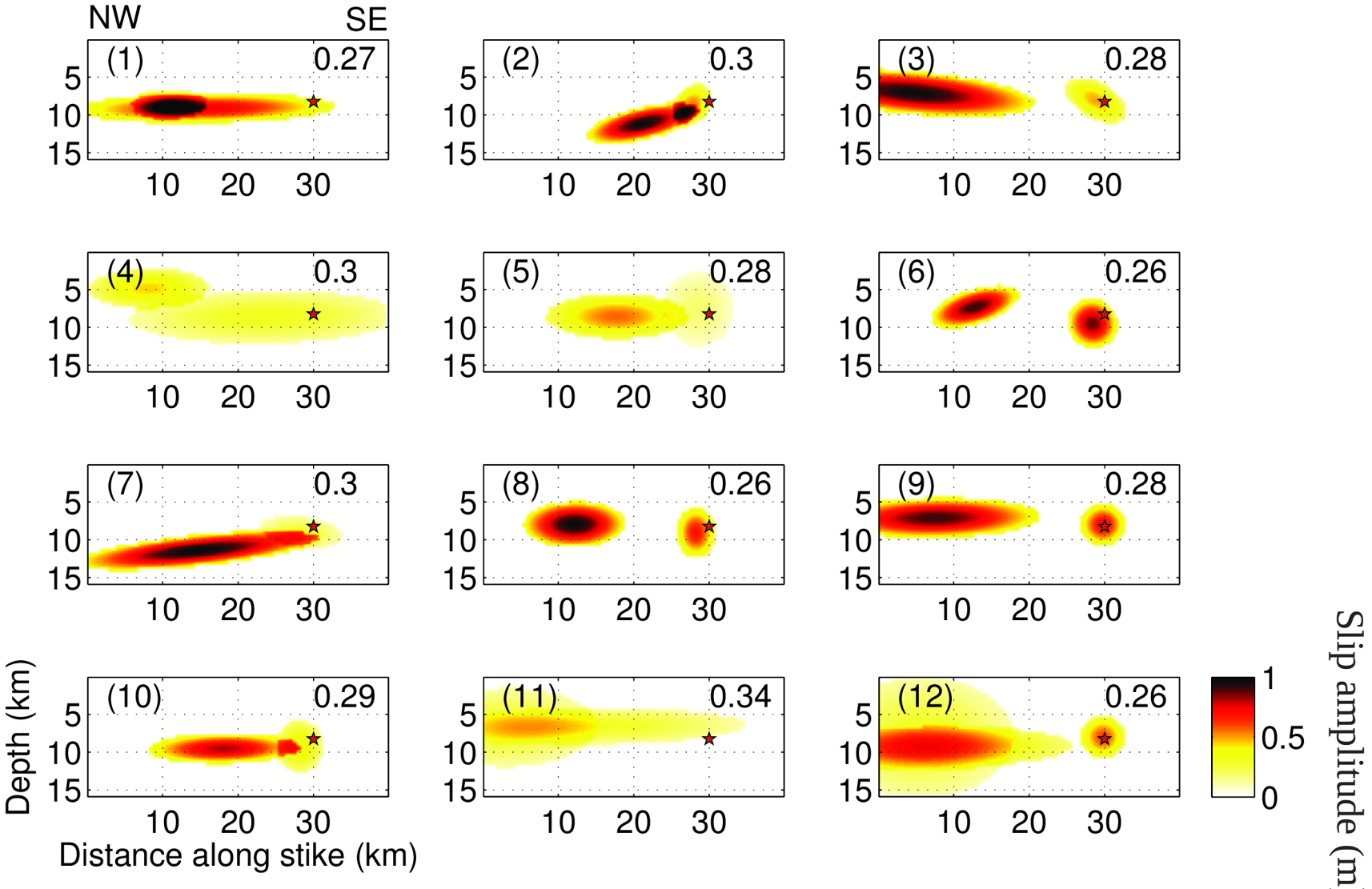

Final slip distribution of the 12 inversions

- Choice of the preferred model:

Final slip distribution of the 12 inversions

- Choice of the preferred model:

  (i) Average model

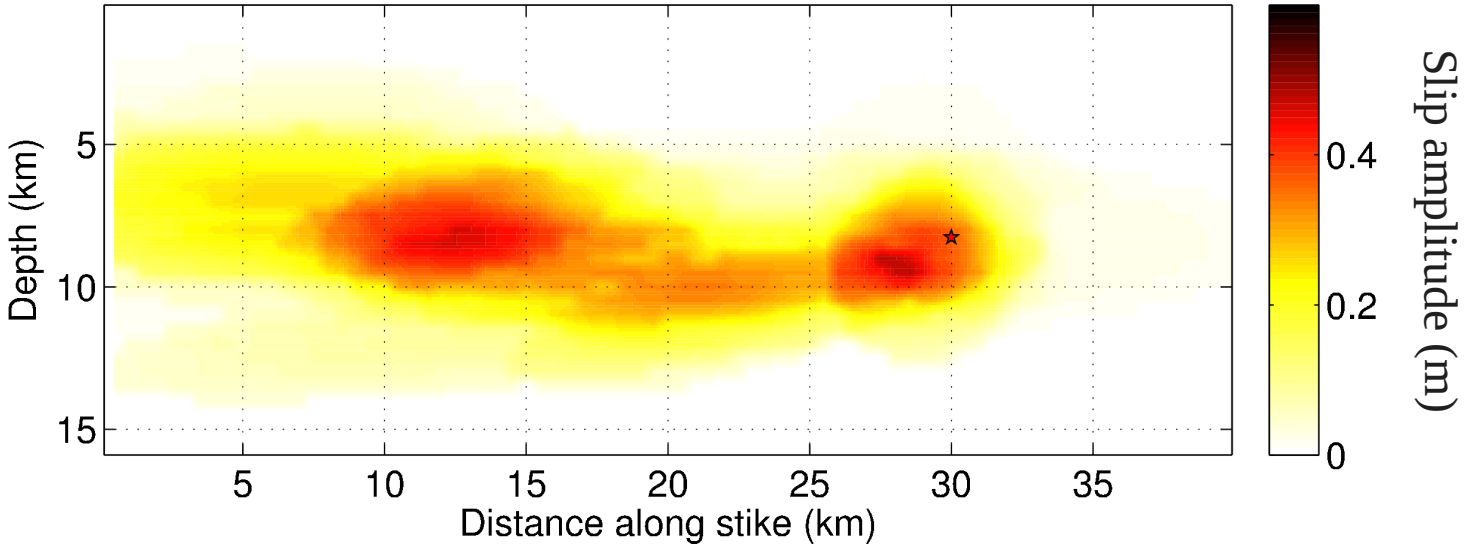

Final slip distribution of the 12 inversions

- Choice of the preferred model:

  (i) Average model

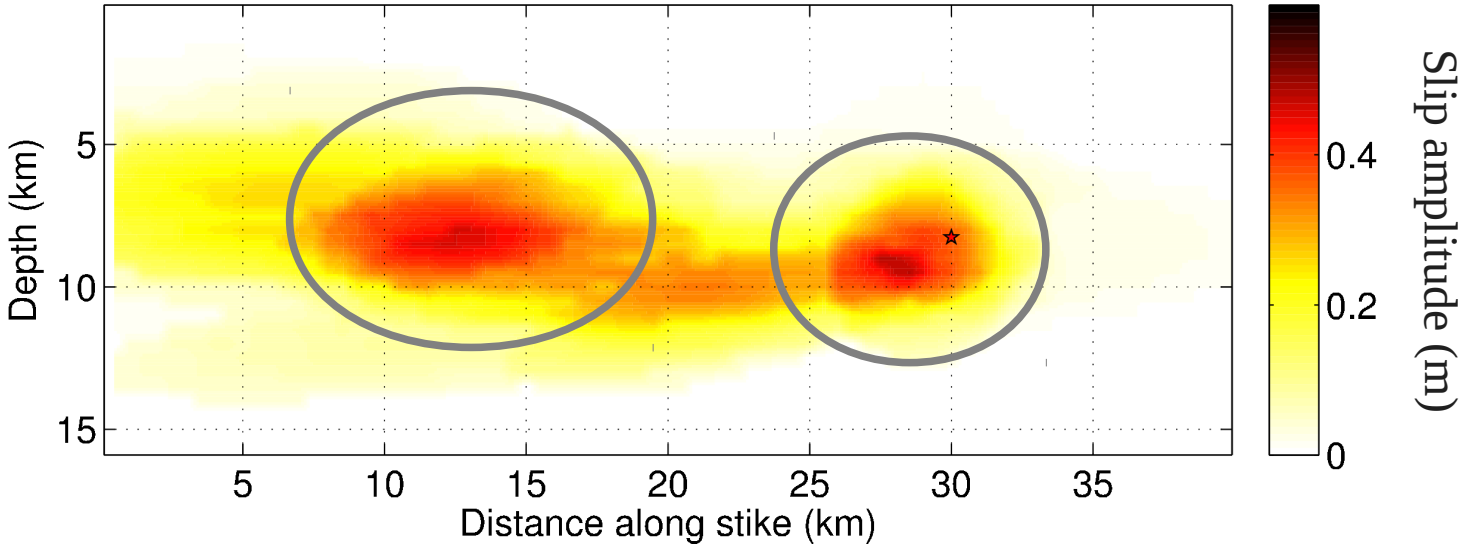

Final slip distribution of the 12 inversions

- Choice of the preferred model:

(i) Average model

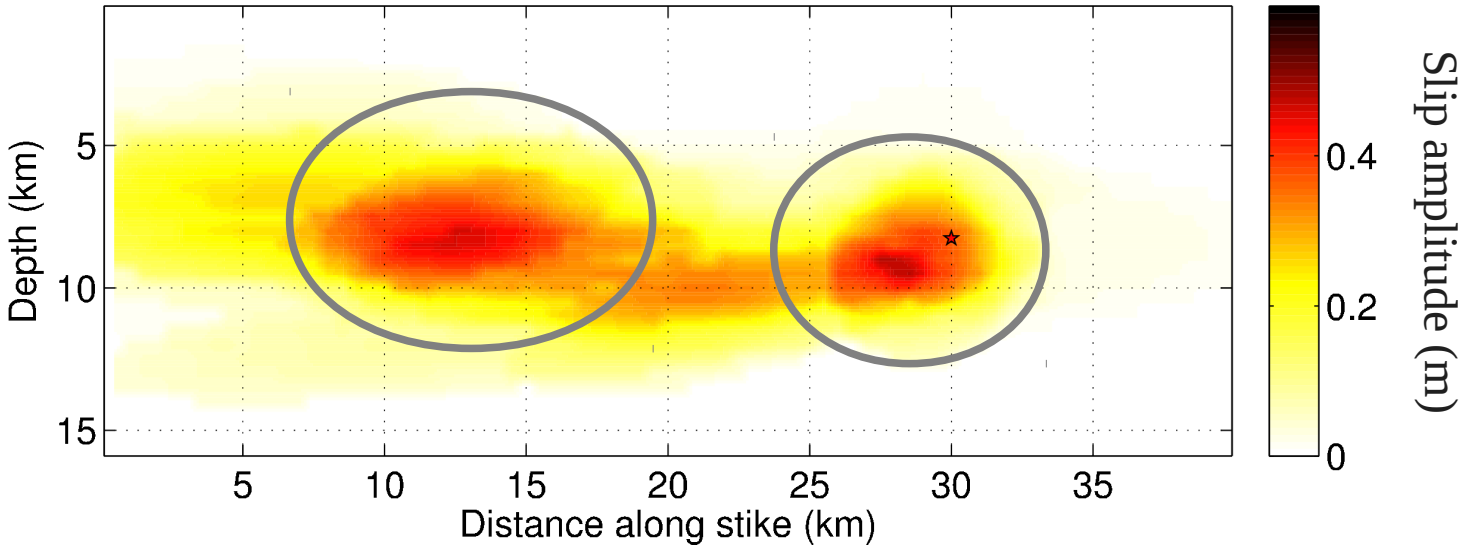

(ii) Comparable moment with the CMT value

Final slip distribution of the 12 inversions

- Choice of the preferred model:

(i) Average model

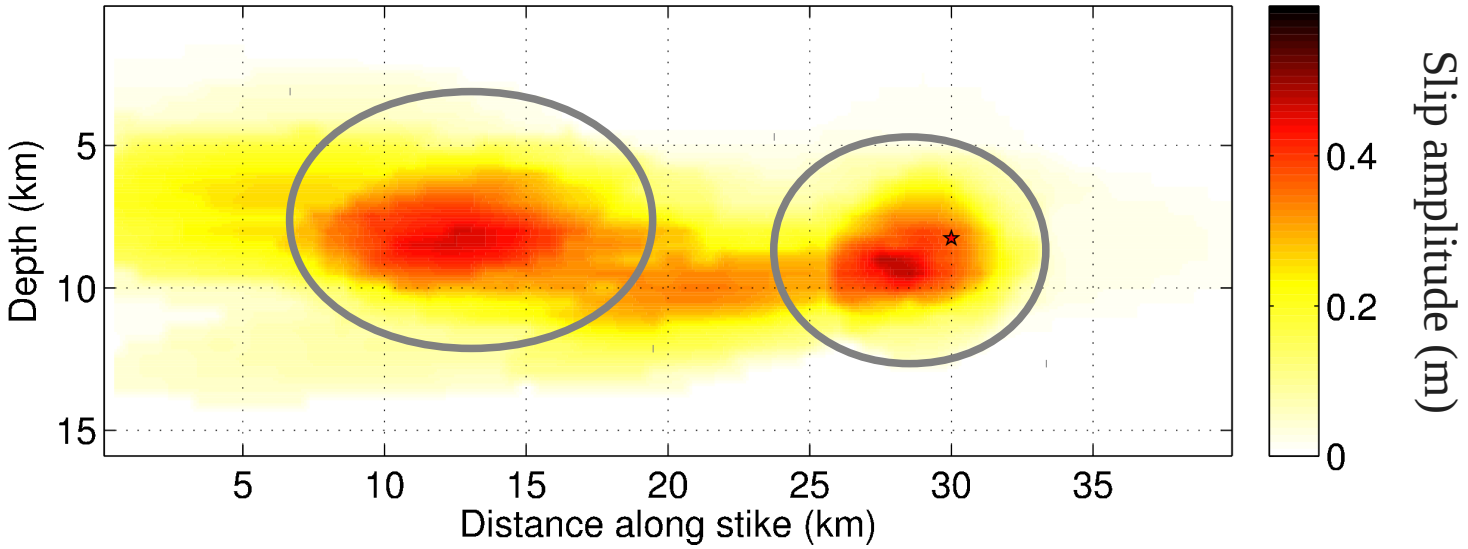

(ii) Comparable moment with the CMT value

(iii) Low global misfit (dig. stations + ana. stations)

Final slip distribution of the 12 inversions

- Choice of the preferred model:

(i) Average model

Inversion #6

Inversion 6 PREFERRED MODEL	Inversion using two disconnected ellipses; No use of *a-priori* conditions; The rise-time and rake were not inverted	Misfit for the digital stations: 0.26; Misfit for the analog stations: 0.56; Moment: 1.21×10^{18} N.m; For this inversion, the rupture is only propagating in the forward direction. It takes 3.2 sec. for the first ellipse to be break at a slow rupture speed of 2.2 km/s. After 3.8 sec. the rupture front reaches the second ellipse. The rupture front slightly accelerates to a speed of 3.1 km/s. After 8.2 sec., the second ellipse is entirely broken. For this inversion, we also calculated the stress drop associated with each ellipse. The stress drop is about 15 MPa for the hypocentral ellipse, and 17 MPa for the second ellipse.

(ii) Comparable moment with the CMT value

(iii) Low global misfit (dig. stations + ana. stations)

Fit to the waveforms

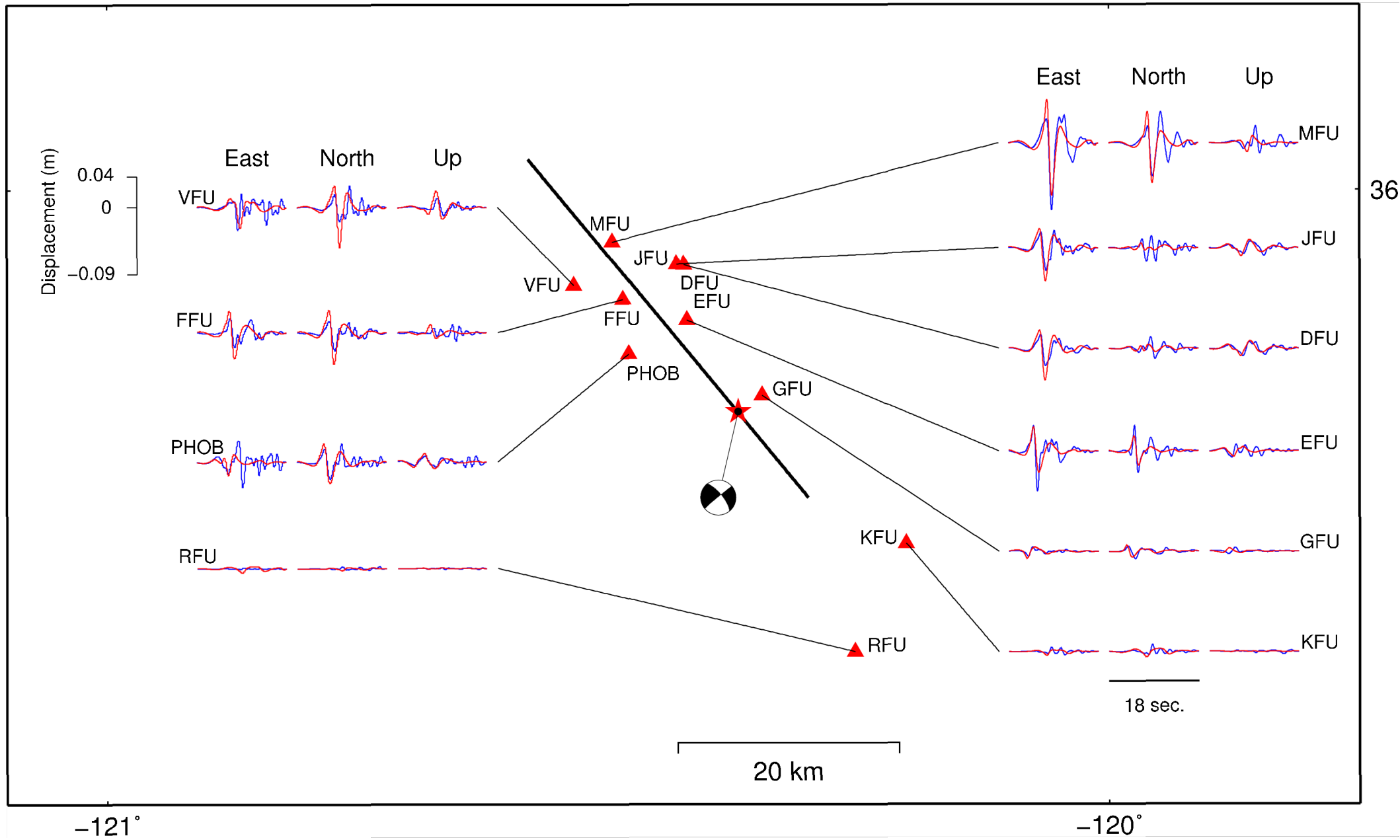

Preferred model

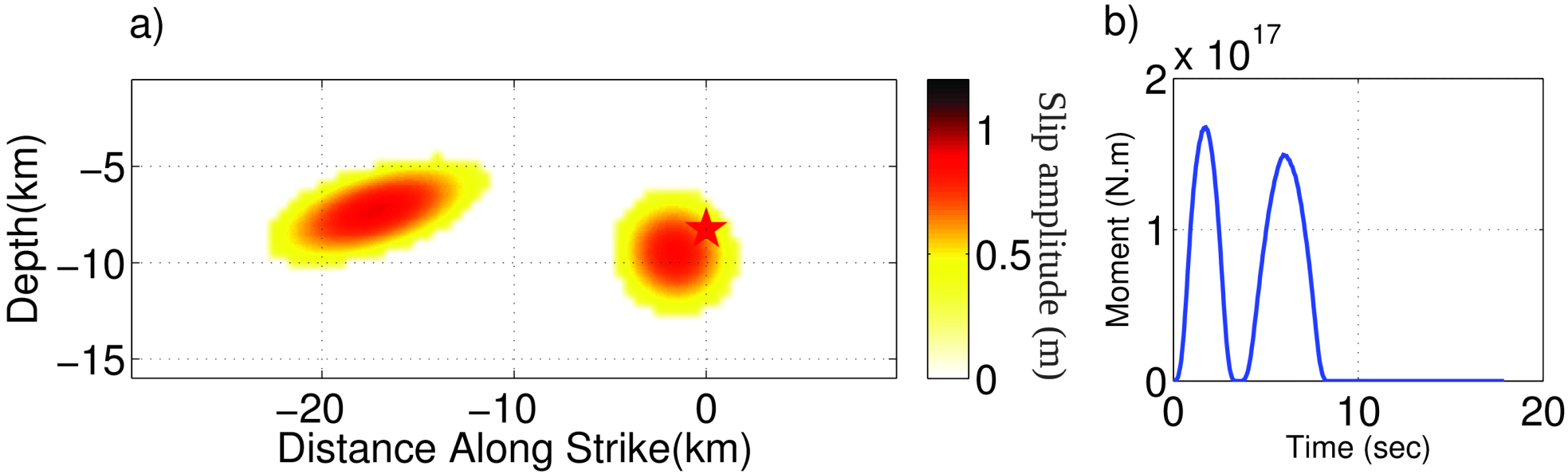

Preferred model

Relation between slip distribution and seismicity prior (1987-2004) the 2004 Parkfield earthquake

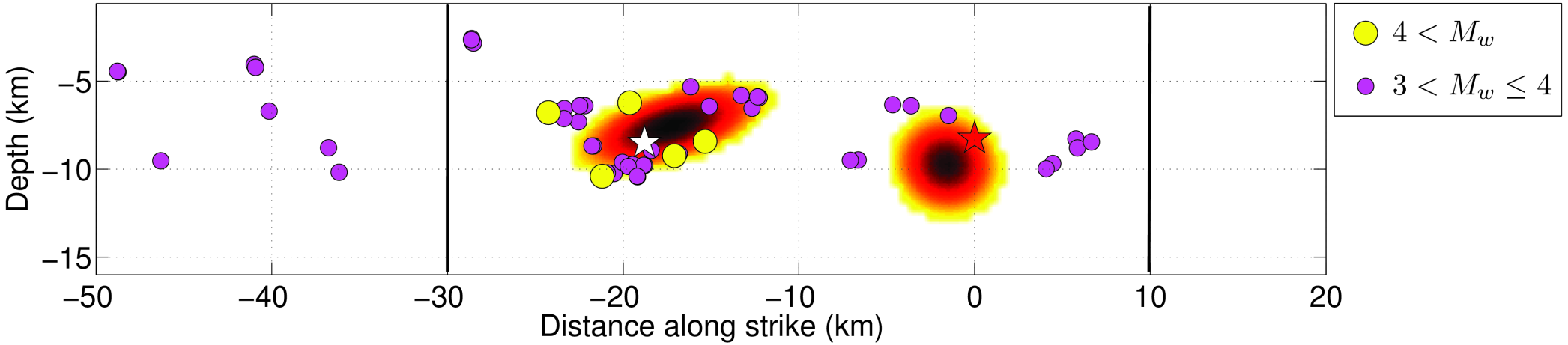

Relation between final slip distribution and aftershocks

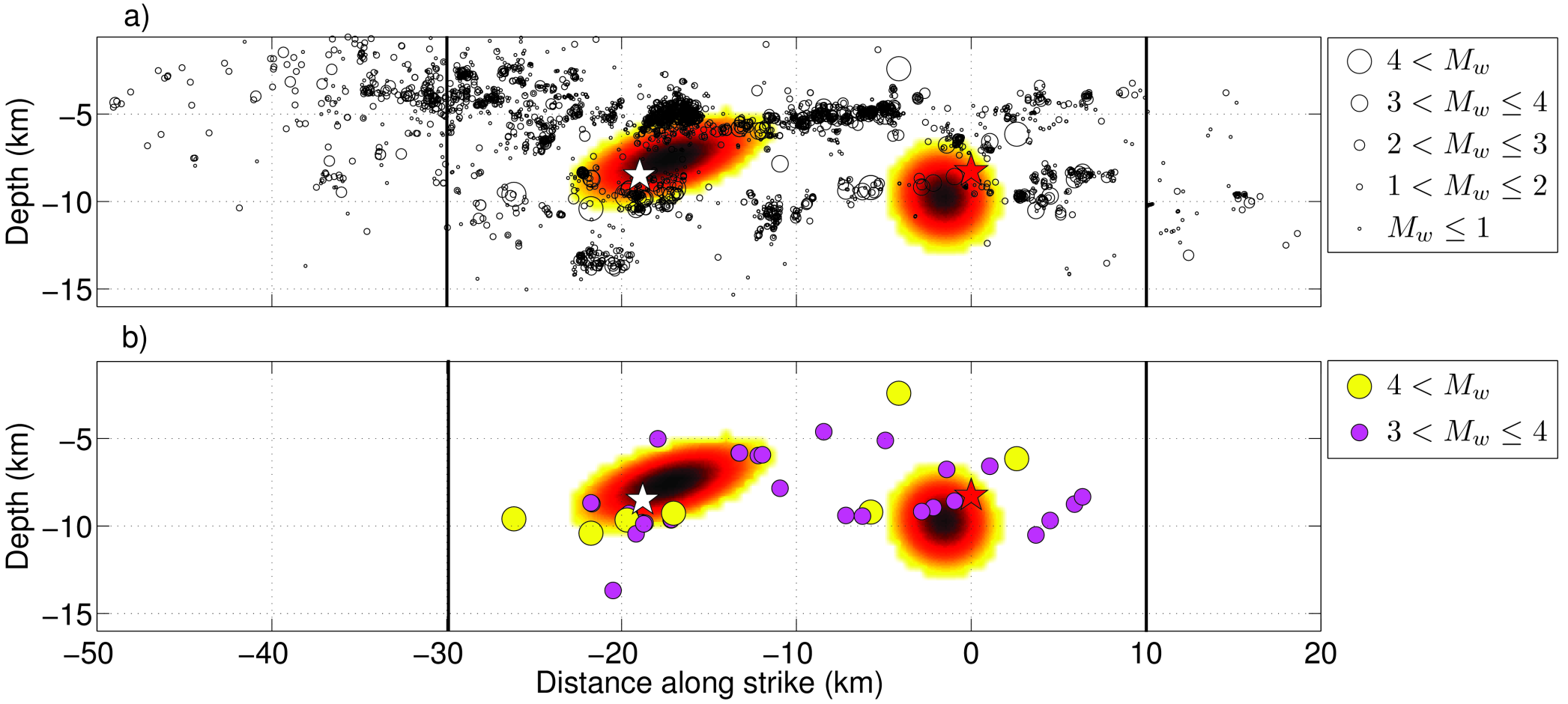

Conclusions

We used a method aimed to map the robust features of an earthquake to infer the source process of the 2004 Parkfield earthquake:

- No slip in the top 5km
- Two major asperities

Our final slip distribution shows coherency with the seismicity prior the 2004 Parkfield earthquake, as well as with its aftershocks:

- Persistent asperity

Thank you

EARTHQUAKE DYNAMICS
IASPEI Assembly, July 22-26, 2013
Gothenburg, Sweden

Convenors:

Cedric Twardzik (Oxford University, UK), Ralph Archuleta (UCSB, USA), Shamita Das (Oxford University, UK) and Raul Madariaga (ENS, Paris).

Improved forecasting of seismic hazard requires a better understanding of the earthquake rupture process. One of the major ways to address this issue is to be able to provide a full dynamic description of the seismic rupture. From this perspective, contributions from a large spectrum of scientific fields are necessary: numerical modelling, laboratory experiments, and geological studies of faults. We welcome innovative studies relating to any aspect of earthquake dynamics. Invited speakers include Ares Rosakis (Caltech) and Satoshi Ide (Japan).

See http://www.iaspei.org/meetings/forthcoming.html#iaspei2013 , for details of abstract deadlines, abstract format, registration details, etc.